THE AMERICAN MINERALOGIST, VOL. 48, JANUARY–FEBRUARY, 1963

CHLORITE POLYTYPISM: II. CRYSTAL STRUCTURE OF A ONE-LAYER CR-CHLORITE

B. E. BROWN[1] AND S. W. BAILEY, *Department of Geology*
University of Wisconsin, Madison, Wisconsin.

ABSTRACT

Purple chlorite from Erzincan, Turkey, contains 9.3% Cr_2O_3 and belongs to space group $C\bar{1}$ with $a=5.338$ Å, $b=9.247$ Å, $c=14.435$ Å, $\beta=97°05'$, $\alpha=\gamma=90°$. The 1-layer structure contains a regular sequence of I*a* type layers, similar to those in vermiculite, in which the brucite sheet is rotated by 180° relative to its orientation in the more common II*b* type layer and is positioned differently on top of the talc sheet. The talc network is distorted by 6° planar rotations of the tetrahedra. The tetrahedral and octahedral cations are ordered in an arrangement that produces local charge balance. All of the octahedral trivalent elements are concentrated preferentially in one site of the brucite sheet so that the locus of excess positive charge is positioned exactly between the excess negative charges associated with the ordered Al tetrahedra of the talc sheets above and below.

INTRODUCTION

The generalized structure of the chlorites was conceived initially by Pauling (1930) and confirmed shortly thereafter by the powder data of McMurchy (1934). More detailed examination of the structures of individual specimens by single crystal methods has revealed a variety of stacking sequences, distortions from geometrically ideal structures, and order-disorder relationships. Part I in the present study of chlorite polytypism (Bailey and Brown, 1962) showed that four different chlorite layer types are theoretically possible and that at least three of these exist in natural specimens. Layers of the same type may be superimposed to form several different semi-random and regular stacking sequences. Six semi-random, twelve regular 1-layer, and an unknown but very large number of regular higher-layer structures are theoretically possible. A semi-random sequence is defined as one in which adjacent layers adopt in irregular sequence any of three permissible stacking positions differing by relative shifts of $\pm\frac{1}{3}$ *b*. A few natural chlorites have been shown to possess regular 1-, 2-, or 3-layer sequences, but most chlorites crystallize with a semi-random sequence involving one particular layer type that is especially stable as a result of minimum cation repulsion and short interlayer OH—O bond lengths. The polytypism of this common type has been studied by Garrido (1949), Brindley, Oughton, and Robinson (1950), and Steinfink (1958a, b, 1961). This paper describes the structure of a specimen having a regular sequence of one of the less common layer types, designated I*a* in the terminology of Bailey and Brown and so far recognized in seven Fe- and Cr-rich chlorites, in six Li-Al cookeites, and in most vermiculities.

[1] Present address Allis-Chalmers Mfg. Co., Dept. 3325, Milwaukee 1, Wisconsin.

Unit Cell and Space Group

We acquired from Dr. R. A. Bell a beautifully crystallized, purple Cr-rich chlorite (kammererite) from the Erzincan province, Turkey. The crystals appear to be hydrothermal in origin, occurring in vugs, veins and other openings in serpentine associated with chromite ore. Certain of these crystals have a regular stacking sequence and give diffraction patterns showing discrete reflections where $k \neq 3n$. A one-layer polytype was the most abundant of the regular stacking specimens that were found and two crystals of this polytype, about 0.15 mm in diameter, were used in collecting the intensity data for the structural determination.

The shape of the unit cell and the magnitudes of the a, b, and c repeat distances were determined first from precession photographs. The pseudohexagonal nature of layer silicates makes it difficult to choose the unique X and Y axes. The three possible Y* axes were examined in three Y*Z* photographs. One photograph has the reflection 020 on a line at right angles to the prominent Z* axis and only on this photograph is the white radiation streak, coincident with Y*, continuous to the center of the film. This unique direction was selected as true Y*.

The c repeat distance on the precession photographs is approximately 14 Å, or $\frac{1}{3}$ the value of the 42 Å repeat observed in the direction normal to the cleavage (Z* direction) on rotation photographs. This relation requires a β angle of 97° for layers with a 14 Å $c \sin \beta$ dimension (Brindley and Robinson, 1951). If the β angle is known, the true X* axis can be identified on an X*Z* precession photograph taken at 90° to the true Y axis. The cell as chosen from precession data is monoclinic in shape with $\alpha = \gamma = 90°$ and $\beta = 97°$. Refined cell parameters determined by the θ method of Weisz, Cochran, and Cole (1948) are $a = 5.338$ Å, $b = 9.247$ Å, $c = 14.435$ Å, and $\beta = 97°05'$. $V = 707.08$ Å^3.

Intensity data for 225 observed reflections were obtained from equatorial Weissenberg photographs taken with Mo Kα radiation about the three axial directions. Multiple film packs were used and the intensities were estimated visually by comparison with a standard multiple scale. Lorentz-polarization corrections were applied, but absorption was neglected because of the small size of the crystals.

The cell is centered on the (001) face, as indicated by systematic absences of the type $h+k=2n+1$ for the general reflections. Laue photographs taken with the x-ray beam perpendicular to the (001) cleavage show trigonal symmetry with regard to certain of the most intense reflections, but not for many of the weaker reflections. No symmetry planes are present. The statistical tests of Howells *et al.* (1950) and of Wilson (1949, 1951) were applied to the corrected intensities to determine the exact space group. The result of the N(z) test is shown in Fig. 1. The distribution of observed intensities for the $h0l$ reflections falls above the theoreti-

cal distribution for a centrosymmetric structure, undoubtedly because most of the atoms in the structure occur at intervals of $\frac{1}{3}$ b and give rise to a hypersymmetry effect. Reflections with $k \neq 3n$ are not influenced by atoms repeating at $\frac{1}{3}$ b and fit the theoretical centrosymmetric distribution much better. The existence of a symmetry center eliminates the possibility of any twofold symmetry axis along Y, since there are no monoclinic space groups containing both a twofold axis and a symmetry center that do not also require a symmetry plane normal to Y. Therefore the symmetry is triclinic, space group $C\bar{1}$, although the cell is of monoclinic shape.

Determination of the Structure

Of the twelve theoretically possible one-layer structures derived by Bailey and Brown (1962) only three belong to space group $C\bar{1}$ and have cell parameters similar to those listed above. These are the polytypes

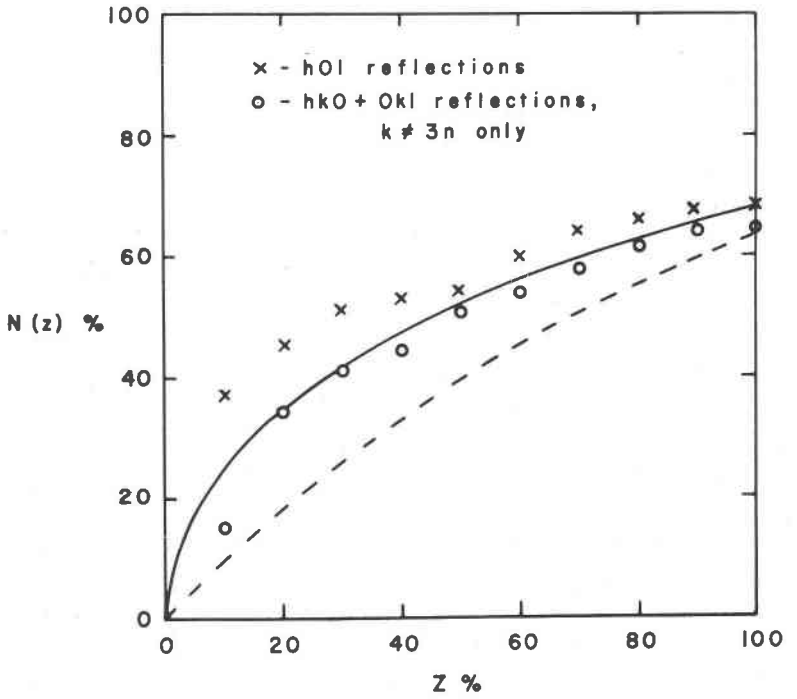

Fig. 1. N(z) statistical test for center of symmetry. Solid line indicates the theoretical intensity distribution for a centrosymmetric structure, dashed line that for a noncentrosymmetric structure. The upper array of points using 109 $h0l$ reflections exhibits hypersymmetry. The lower array using 61 $hk0$ and $0kl$ reflections for which $k \neq 3n$ shows the true symmetry.

I*a*-4, II*a*-3, and II*b*-4. Comparison of the calculated and observed structure amplitudes for the *h*0*l* reflections eliminated all but the type designated I*a*-4. Atomic parameters from this model were used to place the observed structure amplitudes on an absolute scale and to initiate further refinement.

Refinement

Refinement of the structure was carried out using three IBM 650 programs. The Incor I program (Zalkin and Jones, University of California Radiation Laboratory, Berkeley) was used to compute routine corrections for the single crystal Weissenberg data and to place on each reflection card the scattering factors of Berghuis and others (1955) for the different atom types. The output from Incor acts as input to a diagonal term least squares program (Senko and Templeton, Univ. California Radiation Lab., Berkeley) that seeks to minimize the quantity $R = \sum w(F_o - F_c)^2$ by varying the atomic parameters and temperature factors. Only the observed reflections were used, with unit weighting factors (w). A third program (Sindelfungen-Darmstadt-Pittsburgher two-dimensional Fourier program, as modified by R. Shiono of the University of Pittsburgh) was useful in computing F_o and F_o-F_c two-dimensional syntheses. These projections provided information on the nature of chromium ordering and were used to delineate certain atoms that overlapped in all projections. In this latter case an F_o-F_c synthesis was computed in which one of the atoms in question was omitted entirely in the calculation of the F_c values, thereby showing the electron density peak of that atom only in the ρ_o-ρ_c map.

Repeated cycles of least squares and F_o-F_c refinements were carried out for each zone until minimum R values were obtained. At this point the residual shifts in atomic positions were generally less than 0.005 Å in magnitude and random in direction. The average temperature factor determined by the least squares refinement was 1.0. The final overall reliability factor was 10.3%, although this value does not take into account the cation ordering. The final observed and calculated structure amplitudes are listed in Table 1. Table 2 contains the final atomic coordinates. Table 3 contains bond lengths and angles computed from these coordinates.

Discussion of Results

Orientation of the brucite sheet

Part I of the present study of chlorite polytypes described the four basic layer types, I*a*, I*b*, II*a*, and II*b*. The II*b* scheme is the common layer assemblage and is the type analyzed by McMurchy (1934),

Table 1. Observed and Calculated Structure Amplitudes

H	K	L	F_o	F_c	H	K	L	F_o	F_c	H	K	L	F_o	F_c
0	0	1	37	44	6	0	0	44	42	0	6	4	56	58
0	0	2	97	74	6	0	1	19	-20	0	6	5	32	36
0	0	3	121	-119	6	0	2	28	36	0	6	6	52	46
0	0	4	162	150	6	0	3	20	9	0	6	7	26	-26
0	0	5	97	99	6	0	4	20	21	0	6	8	28	-32
0	0	6	21	-15	6	0	6	14	-7	0	6	10	80	82
0	0	7	85	-74	6	0	8	43	41	0	6	11	35	36
0	0	8	25	-26	6	0	9	27	20	0	6	12	66	60
0	0	9	29	34	6	0	10	45	45	0	6	13	38	-35
0	0	10	93	95	6	0	11	23	-21	0	6	14	56	58
0	0	11	21	20	6	0	12	33	32	0	6	16	67	70
0	0	12	93	89	6	0	14	55	47	0	6	-2	96	96
0	0	13	24	-17	6	0	-2	102	103	0	6	-3	55	-56
0	0	14	82	78	6	0	-3	19	14	0	6	-4	56	55
0	0	16	90	83	6	0	-4	47	46	0	6	-5	32	40
0	0	19	43	-33	6	0	-5	39	-42	0	6	-6	54	50
0	0	21	33	18	6	0	-6	40	30	0	6	-7	26	-26
0	0	22	24	22	6	0	-8	40	33	0	6	-8	28	-35
0	0	26	53	41	6	0	-9	35	-27	0	6	-10	78	81
2	0	0	108	102	6	0	-12	57	56	0	6	-11	35	34
2	0	1	34	51	6	0	-14	30	31	0	6	-12	64	60
2	0	2	199	199	6	0	-15	16	-20	0	6	-13	32	-34
2	0	3	29	-25	6	0	-16	47	47	0	6	-14	56	58
2	0	4	152	155	6	0	-18	42	37	0	6	-16	67	68
2	0	5	28	-18	8	0	0	49	46	0	8	0	12	7
2	0	6	161	178	8	0	2	34	28	0	8	-7	17	22
2	0	7	27	31	8	0	4	60	46	0	12	0	92	92
2	0	8	47	41	8	0	7	18	-16	0	12	2	21	26
2	0	9	62	-62	8	0	-1	16	12	0	12	3	37	-37
2	0	11	33	34	8	0	-2	29	24	0	12	4	21	34
2	0	12	57	56	8	0	-3	29	-23	0	12	5	22	19
2	0	16	74	78	8	0	-10	35	37	0	12	6	17	18
2	0	17	15	24	8	0	-12	56	42	0	12	7	22	-21
2	0	18	49	50	10	0	4	27	20	0	12	10	40	40
2	0	-1	43	-36	10	0	6	33	28	0	12	12	34	31
2	0	-2	69	-80	10	0	-6	27	29	0	12	14	43	38
2	0	-3	23	-14	10	0	-10	38	32	0	12	16	44	36
2	0	-4	62	58	0	2	0	50	38	0	12	-2	21	27
2	0	-5	55	60	0	2	1	58	-51	0	12	-3	21	-25
2	0	-6	53	41	0	2	2	41	-54	0	12	-4	37	36
2	0	-7	74	-65	0	2	3	8	12	0	12	-5	22	16
2	0	-8	120	126	0	2	4	53	57	0	12	-7	17	-18
2	0	-9	53	62	0	2	6	19	-21	0	12	-10	40	33
2	0	-10	171	179	0	2	7	21	-22	0	12	-12	42	38
2	0	-11	31	-36	0	2	9	13	21	0	12	-14	35	32
2	0	-12	40	38	0	2	-1	48	62	0	12	-16	36	40
2	0	-13	24	-21	0	2	-2	14	6	0	18	0	39	41
2	0	-14	71	72	0	2	-3	66	-69	1	1	0	28	18
2	0	-15	13	13	0	2	-4	13	-21	1	3	0	43	-38
2	0	-17	35	-28	0	2	-5	10	14	1	5	0	48	-45
2	0	-20	50	42	0	2	-6	45	44	1	9	0	41	-40
2	0	-22	24	28	0	2	-9	23	-27	1	-1	0	82	-74
2	0	-24	25	36	0	4	0	11	-9	1	-3	0	43	-40
4	0	0	43	-50	0	4	1	24	-16	1	-7	0	35	-35
4	0	1	15	19	0	4	2	31	24	1	-9	0	41	-38
4	0	2	85	81	0	4	5	46	-51	2	2	0	23	-30
4	0	5	40	-36	0	4	6	32	27	2	4	0	30	-33
4	0	6	100	106	0	4	7	27	34	2	6	0	89	89
4	0	7	30	36	0	4	9	59	-61	2	12	0	40	39
4	0	8	102	102	0	4	11	28	32	2	-2	0	11	13
4	0	9	26	-24	0	4	12	38	32	2	-4	0	46	42
4	0	10	46	44	0	4	13	17	-16	2	-6	0	92	90
4	0	12	34	38	0	4	-1	24	30	2	-12	0	46	38
4	0	18	34	38	0	4	-2	11	2	3	1	0	26	30
4	0	-1	63	-62	0	4	-3	41	-43	3	5	0	35	-36
4	0	-2	89	87	0	4	-5	30	33	3	7	0	18	24
4	0	-3	60	69	0	4	-6	32	32	3	-1	0	40	-33
4	0	-4	115	119	0	4	-7	38	-41	3	-3	0	14	7
4	0	-5	57	-58	0	4	-8	32	-34	3	-5	0	16	8
4	0	-6	78	86	0	4	-10	46	42	3	-9	0	20	19
4	0	-8	122	130	0	4	-12	38	-38	4	-2	0	16	-24
4	0	-11	25	-31	0	6	0	190	210	5	3	0	32	31
4	0	-14	28	29	0	6	1	9	10	5	-3	0	37	36
4	0	-18	55	52	0	6	2	90	91	6	-6	0	22	18
4	0	-20	53	49	0	6	3	52	-57	8	-6	0	20	26

TABLE 2. ATOMIC COORDINATES OF THE ERZINCAN I*a*-4 Cr-CHLORITE

	x	y	z
2 M_I (Mg)	0.0	0.0	0.0
4 M_{II} (Mg)	−0.001	0.333	0.002
4 M_{III} (Mg)	0.003	0.166	0.504
2 M_{IV} ($Cr_{0.7}Al_{0.2}Mg_{0.1}$)	0.0	0.5	0.5
4 T_I ($Si_{0.6}Al_{0.4}$	0.400	0.001	0.191
4 T_{II} ($Si_{0.9}Al_{0.1}$)	0.894	0.167	0.191
4 O_I	0.360	−0.004	0.075
4 O_{II}	0.860	0.171	0.076
4 $(OH)_I$	0.381	0.333	0.074
4 O_{III}	0.133	0.065	0.232
4 O_{IV}	0.645	0.100	0.232
4 O_V	0.931	0.328	0.234
4 $(OH)_{II}$	0.154	−0.002	0.432
4 $(OH)_{III}$	0.129	0.339	0.428
4 $(OH)_{IV}$	0.653	0.164	0.428

Garrido (1949), Brindley *et al.* (1950), and Steinfink (1958a, b, 1961). The Erzincan specimen has a I*a* layer type in which the brucite sheet is rotated 180° relative to that in the II*b* arrangement and is positioned differently on top of the talc sheet. This structure produces a pattern of $k=3n$ reflections different from the common II*b* chlorite pattern described by Brindley *et al.* (1950). This difference is illustrated diagrammatically in Fig. 2, in which the left hand portion of a rotation photograph from the Erzincan I*a* specimen is matched with a right hand portion from a II*b* penninite. The structural difference is illustrated schematically in Figure 3.

Distortion of the hexagonal networks

An ideal hexagonal network was assumed for the talc sheet at the start of refinement. The atoms that shifted by the largest amount, 0.17 Å average, from the idealized positions during the refinement are the triads of oxygen atoms forming the base of each tetrahedron. The tetrahedra are rotated in opposite directions in the (001) plane by an average angle of 6.2°, distorting the ideal hexagonal configuration of the oxygen net to an approximate ditrigonal net. The individual oxygen atom shifts have components such that large and small tetrahedra are created due to ordering of the cations. Figure 4 shows the form of the resulting distorted net.

The direction of distortion of the talc oxygen network is such that the basal oxygens in both tetrahedral sheets rotate towards the positions of

TABLE 3. INTERATOMIC DISTANCES AND ANGLES[1]

(1) Tetrahedral distances in Å (*=apical oxygen)

		around T_I	around T_{II}
T_I—O_I* = 1.66$_2$	T_{II}—O_{II}* = 1.64$_8$	O_I*—O_{III} = 2.77$_3$	O_{II}*—O_{III} = 2.71$_0$
T_I—O_{III} = 1.71$_5$	T_{II}—O_{III} = 1.63$_7$	O_I*—O_{IV} = 2.74$_3$	O_{II}*—O_{IV} = 2.73$_1$
T_I—O_{IV} = 1.64$_6$	T_{II}—O_{IV} = 1.64$_2$	O_I*—O_V = 2.75$_9$	O_{II}*—O_V = 2.69$_1$
T_I—O_V = 1.71$_7$	T_{II}—O_V = 1.61$_6$	O_{III}—O_{IV} = 2.75$_2$	O_{III}—O_{IV} = 2.62$_5$
		O_{III}—O_V = 2.70$_6$	O_{III}—O_V = 2.66$_2$
Mean = 1.68$_5$	Mean = 1.63$_6$	O_{IV}—O_V = 2.76$_4$	O_{IV}—O_{IV} = 2.60$_1$
		Mean = 2.75$_0$	Mean = 2.67$_0$

(2) Octahedral distances in Å (ξ=edge shared by two octahedra)

M_I—O_I = 2.08$_6$×2	M_{II}—O_I = 2.03$_1$, 2.12$_3$	M_{III}—$(OH)_{II}$ = 2.01$_2$, 2.08$_6$	M_{IV}—$(OH)_{II}$ = 1.98$_2$×2
M_I—O_{II} = 2.11$_3$×2	M_{II}—O_{II} = 2.03$_3$, 2.10$_0$	M_{III}—$(OH)_{III}$ = 2.08$_5$, 2.09$_7$	M_{IV}—$(OH)_{III}$ = 1.98$_7$×2
$M_I(OH)_I$ = 2.02$_4$×2	M_{II}—$(OH)_I$ = 2.03$_6$, 2.17$_2$	M_{III}—$(OH)_{IV}$ = 2.04$_7$, 2.08$_1$	M_{IV}—$(OH)_{IV}$ = 2.06$_3$×2
Mean = 2.07$_4$	Mean = 2.08$_2$	Mean = 2.06$_8$	Mean = 2.01$_1$

around M_I	around M_{II}	around M_{III}
O_I—O_{II} = 3.12$_3$×2, 2.80$_8$×2$^\xi$	O_I—O_{II} = 3.00$_5$, 3.12$_0$, 2.80$_8^\xi$	$(OH)_{II}$—$(OH)_{III}$ = 3.15$_6$, 3.15$_9$, 2.66$_8^\xi$
O_I—$(OH)_I$ = 2.96$_7$,×2, 2.84$_6$×2$^\xi$	O_I—$(OH)_I$ = 3.16$_5$, 3.11$_8$, 2.84$_6^\xi$	$(OH)_{II}$—$(OH)_{IV}$ = 3.08$_9$, 3.07$_8$, 2.62$_2^\xi$
O_{II}—$(OH)_I$ = 3.12$_8$×2, 2.70$_9$×2$^\xi$	O_{II}—$(OH)_I$ = 3.16$_2$, 2.96$_1$, 2.709$^\xi$	$(OH)_{III}$—$(OH)_{IV}$ = 3.23$_2$, 3.01$_2$, 2.71$_3^\xi$
around M_{IV}	O_I—O_I = 2.78$_0^\xi$	$(OH)_{II}$—$(OH)_{II}$ = 2.71$_2^\xi$
$(OH)_{II}$—$(OH)_{III}$ = 2.93$_8$×2, 2.66$_8$×2$^\xi$	O_{II}—O_{II} = 2.77$_4^\xi$	$(OH)_{III}$—$(OH)_{III}$ = 2.83$_5^\xi$
$(OH)_{II}$—$(OH)_{IV}$ = 3.08$_1$×2, 2.62$_2$×2$^\xi$	$(OH)_I$—$(OH)_I$ = 2.85$_3^\xi$	$(OH)_{IV}$—$(OH)_{IV}$ = 2.719$^\xi$
$(OH)_{III}$—$(OH)_{IV}$ = 3.00$_3$×2, 2.71$_3$×2$^\xi$		

[1] The third decimal place listed in (1), (2) and (3) is not significant and is included only to show the exact figures used in deriving the mean values.

TABLE 3.—(*Continued*)

(3) O—(OH) distances in Å between talc and brucite sheets

O_{III}—$(OH)_{II}$ = $2.94_1 \times 2$
O_{IV}—$(OH)_{IV}$ = $2.88_6 \times 2$
O_V—$(OH)_{III}$ = $2.87_1 \times 2$

Mean = 2.89_9

(4) Standard deviations in Å

	σ_x		σ
$T_{I,II}$	= 0.012	($T_{I,II}$—O)	= 0.019
$M_{II,III}$	= 0.012	($M_{II,III}$—O)	= 0.019
$M_{I,IV}$	= 0.000	($M_{I,IV}$—O)	= 0.015
O, OH	= 0.015	(O—O, OH)	= 0.021

(5) Tetrahedral bond angles in degrees (*=apical oxygen)

O_I*—T_I—O_{III} = 110.4	O_{II}*—T_{II}—O_{III} = 110.8	T_I—O_{III}—T_{II} = 136.1
O_I*—T_I—O_{IV} = 112.1	O_{II}*—T_{II}—O_{IV} = 112.7	T_I—O_{IV}—T_{II} = 136.3
O_I*—T_I—O_V = 109.5	O_{II}*—T_{II}—O_V = 111.0	T_I—O_V—T_{II} = 135.8
O_{III}—T_I—O_{IV} = 110.0	O_{III}—T_{II}—O_{IV} = 106.4	Mean = 136.1
O_{III}—T_I—O_V = 104.1	O_{III}—T_{II}—O_V = 109.4	
O_{IV}—T_I—O_V = 110.6	O_{IV}—T_{II}—O_V = 106.4	
Mean = 109.4	Mean = 109.4	

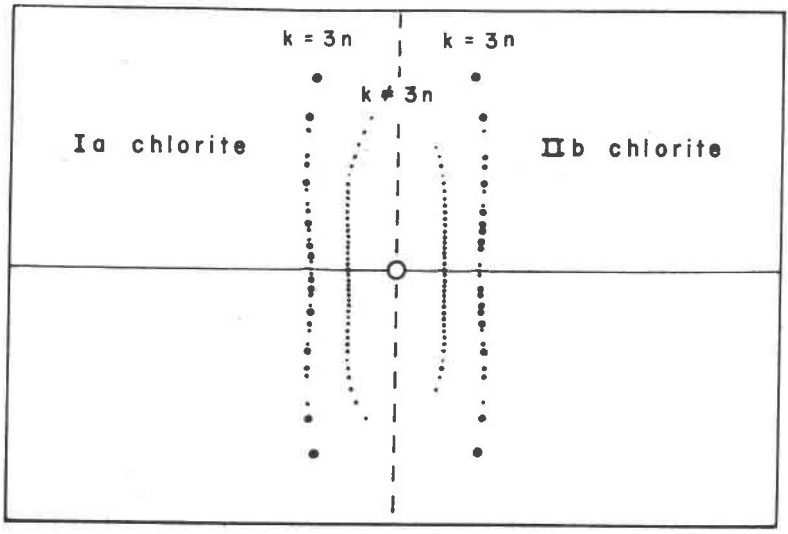

FIG. 2. Schematic view of the two innermost row lines in rotation photographs taken about the cleavage normal, illustrating the intensity differences for I*a* and II*b* 1-layer chlorites.

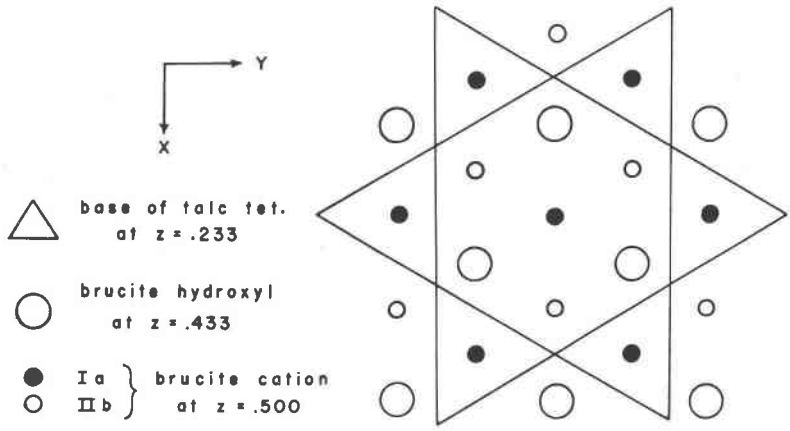

FIG. 3. Normal projection onto (001) of the tetrahedra of an ideal hexagonal ring in the upper half of the talc sheet plus the superimposed brucite sheet. The I*a* and II*b* layers differ as to positions of the brucite cations. The upper plane of brucite hydroxyls (not shown) will also differ because it must be emplaced to provide octahedral coordination about the cation sites occupied.

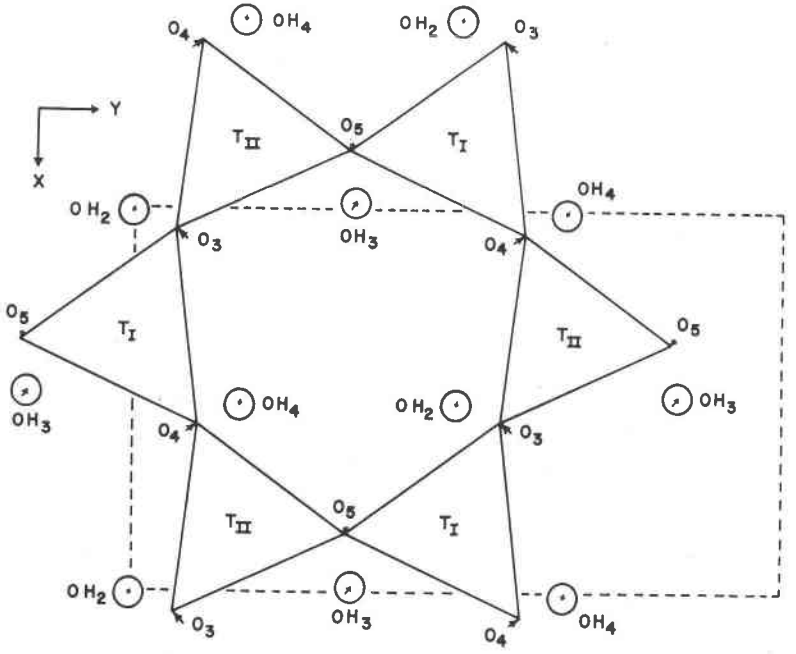

FIG. 4. Ditrigonal tetrahedral ring in Erzincan chlorite after 6° rotation of tetrahedra. Adjacent talc oxygens and brucite hydroxyls have shifted towards one another in the (001) plane, by amounts indicated by the small arrows, to provide shorter O—OH interlayer contacts.

the talc octahedral cations and also towards the nearest hydroxyls in the adjacent brucite sheets (Fig. 4). The brucite hydroxyls in turn shift slightly, 0.07 Å average, towards the basal oxygens to give shorter O—OH contacts between the talc and brucite sheets. The latter shifts have the effect of rotating the upper and lower hydroxyl triads in the octahedron about each brucite cation by an average angle of 1.5°. At the same time large and small octahedra are provided to accommodate the segregation of the divalent and trivalent brucite cations. The distortion of the brucite sheet, however, is small relative to that of the talc sheet.

The phenomenon of tetrahedral rotation is characteristic of layer silicate structures. As noted by Bradley (1959), it is apparently a result of the misfit between octahedral and tetrahedral sheets. In most layer silicates the octahedral sheet is smaller than the tetrahedral sheet and tetrahedral rotation is a mechanism whereby the tetrahedral sheet shrinks to a size more compatible with the dimensions of the octahedral sheet.

Radoslovich (1961) gives a simple expression

$$\alpha = \cos^{-1}\left[b(\text{obs})/b(\text{tetr})\right] \qquad (1)$$

relating α, the angle of tetrahedral rotation, to the observed and the ideal tetrahedral b parameters. We have found that the ideal b parameter for an unconstrained tetrahedral sheet at maximum extension, b (tetr) for case $\alpha = 0°$, can be derived geometrically from the basal oxygen-oxygen distances in the tetrahedral sheet by

$$b(\text{tetr}) = (\text{A} + \text{B}) \cos (30° + \alpha) + (\text{A} + \text{B}) \cos (30° - \alpha) \qquad (2)$$

or

$$b(\text{tetr}) = (\text{A} + \text{B})\sqrt{3} \qquad (\text{for } \alpha = 0°) \qquad (3)$$

where A and B refer to the average of the basal oxygen-oxygen distances in tetrahedra of different sizes. Figure 5 shows the variation of b (tetr) with tetrahedral composition, as derived using equation (3) and the observed basal oxygen-oxygen distances in a number of individual layer silicate structures. Table 4 lists the α angles calculated by substitution of these individual b (tetr) values into equation (1). We have confirmed that the calculated α values agree quite closely with the observed values, as they must if the cell dimension and atomic coordinate data are internally consistent. Equation (3) can be extended to cover layer silicates for which the structures have not been determined by assuming the basal oxygen-oxygen distances to vary linearly with tetrahedral composition from 2.610 Å at Si_4Al_0 to 2.734 Å at Si_2Al_2. These are the values predicted by the line of best fit in Fig. 5, although b (tetr) for Si_4Al_0 is somewhat uncertain because of the deviation of the two points representing kaolinite and dickite. Substitution of b (tetr) into equation (1) then allows prediction of α, provided that b (obs) $< b$ (tetr) and that there are no extenuating steric factors that might override the simple size considerations used here.

TABLE 4. CALCULATED AND OBSERVED TETRAHEDRAL ROTATION ANGLES

	b (obs)	b (tetr)	α (calc)	α (obs)[1]
Xanthophyllite (Takéuchi and Sadanaga, 1959)	9.00 Å	9.776 Å	23.0°	23.1°
Prochlorite (Steinfink, 1961)	9.30	9.429	9.5	8.4
Amesite (Steinfink and Brunton, 1956)	9.20	9.426	12.6	12.4
Corundophyllite (Steinfink, 1958b)	9.27	9.346	7.3	7.6
Cr-chlorite (this paper)	9.427	9.301	6.2	6.2
$2M_1$ muscovite (Radoslovich, 1960)	8.996	9.235	13.1	13.1
Vermiculite (Mathieson, 1958)	9.262	9.287	4.2	4.4
Kaolinite (Drits and Kashaev, 1960)	8.93	9.107	11.3	11.1
Dickite (Newnham, 1961)	8.940	9.017	7.5	7.3

[1] Obtained by calculation of the O_b-O_b-O_b angles from the published atomic coordinates and cell dimensions.

The ideal b parameter for an unconstrained tetrahedral sheet also could be calculated from the observed (Si, Al)—O distances. It can be shown for a hexagonal net of regular tetrahedra that

$$b(\text{tetr}) = 5.657(\text{T—O}_b) \tag{4}$$

where T—O_b is an average of the tetrahedral bonds to the three basal oxygens for all the tetrahedra in the unit cell. In practice this expression gives b (tetr) values (shown in dashed line in Fig. 5) slightly larger than

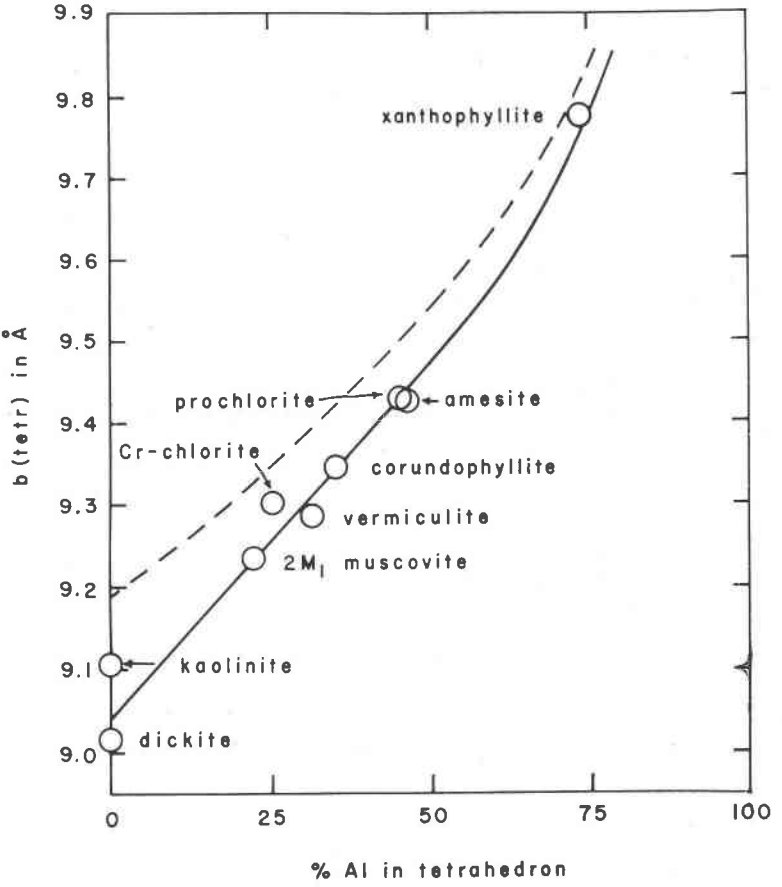

FIG. 5. Ideal b parameter for an undistorted tetrahedral sheet. Values calculated from observed basal O—O distances in individual structures are plotted against average tetrahedral composition as allocated from chemical analysis of the bulk sample. Selected line of best fit is essentially linear from 9.04 Å at Al_0 to 9.47 Å at $Al_{0.5}$. Dashed line curve was derived from T—O_b distances in the same structures, assuming regular tetrahedral shapes. The individual points are not shown for this curve.

those calculated from the basal oxygen-oxygen distances, probably because of deviation of the tetrahedra from regular tetrahedral shapes and variations in the angles linking adjacent tetrahedra.

A survey of the literature on layer silicates shows a linear variation of the mean of all four T—O distances in a tetrahedron with change in tetrahedral composition. The evidence for this variation is being published separately (Smith and Bailey, 1963). The shapes of the tetrahedra tend to vary with tetrahedral composition also. At a low Al-content the $T—O_b$ distances (to the basal, shared oxygens) tend to be shorter than the $T—O_a$ distances (to the apical, unshared oxygen). With increasing Al-content the $T—O_b$ bonds increase in length at a faster rate than the $T—O_a$ bond, with the result that at high Al concentrations $T—O_b$ may be longer than $T—O_a$ (Fig. 6). This effect is illustrated most strikingly by comparing individual bond lengths in tetrahedra of ordered structures, as in $2M_1$ muscovite, monoclinic prochlorite, and Erzincan Cr-chlorite. The basal oxygens in the Al-rich tetrahedra tend to move away from the tetrahedral cation and towards the adjacent interlayer material as a result of the relative weakening of the tetrahedral bond. Despite the general trend, however, there is a considerable scatter of points in Fig. 6 that can not be attributed entirely to experimental error. These variations are believed to represent the effect of other factors on the individual bond lengths, in addition to cation size and to the relative attractive forces of the tetrahedral, octahedral, and interlayer charges. The individual bond lengths are undoubtedly affected also by such factors as cation-cation and anion-anion repulsion, by shortening of shared octahedral edges, and by the need for articulation with interlayer cations or sheets of different sizes.

Chemical variability

Correlation of the Erzincan structural data with the chemical analyses has been made difficult by chemical variability between different grains within the sample. Variation between different grains is indicated both by partial chemical analyses of different size fractions and by refractive index measurements. The refractive indices of three different grains from our sample are listed in Table 5, along with the index of a grain (crystal 4) from a different sample from Erzincan used by Lapham (1958, sample 24) in his study of Cr-chlorites. Crystal 1 is one of the two crystals used for intensity measurements in our study. These grains were measured by double variation techniques using the quartz O ray to standardize the equipment. The specimens are sensibly uniaxial. In addition, the slopes of the dispersion curves for α and γ are significantly different, causing them to intersect. In the crystal used for the structural analysis this intersec-

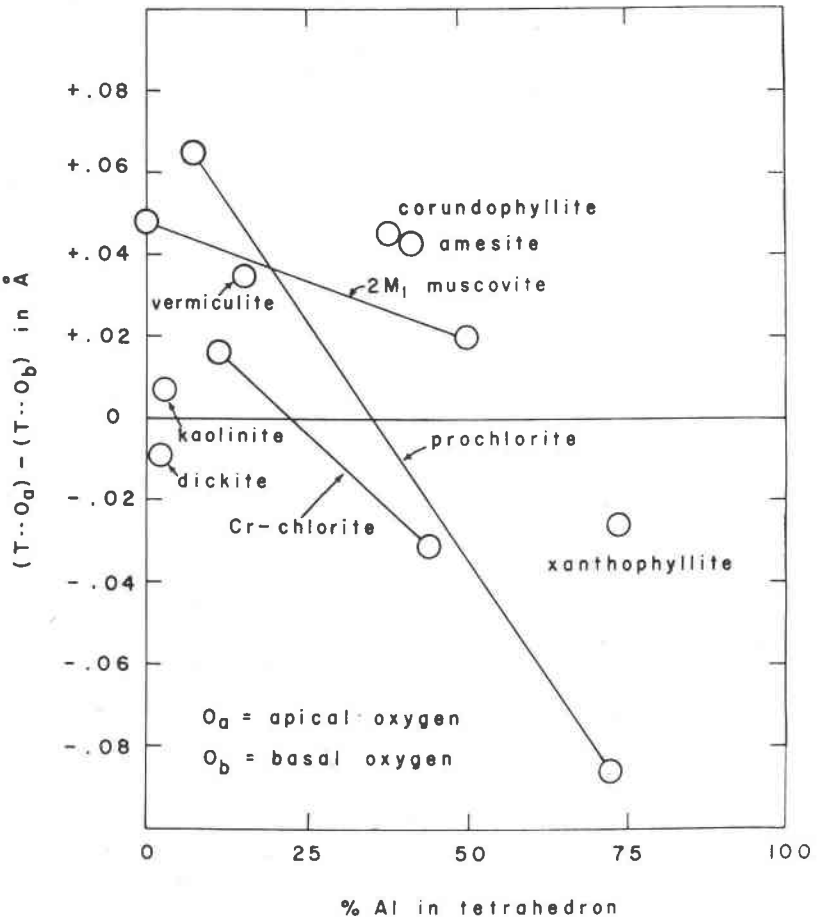

FIG. 6. Variation of tetrahedral shape with composition. The tetrahedral bond to the apical oxygen tends to be longer than those to the basal oxygens at Si-rich compositions, but shorter at Al-rich compositions. Solid lines connect ordered tetrahedra of different compositions in the same structure. Tetrahedral composition was derived from a linear mean bond length graph from Si—O=1.62 Å to Al—O=1.77 Å.

tion occurs at about the sodium D line (589 mu) and at this wave length the crystal is isotropic. The measurements were made by Dr. H. H. Bostock and Mr. G. L. LaBerge. They comment that within a single grain different edges have slightly different refractive indices. The slope of Lapham's plot of the γ refractive index variation with Cr_2O_3 content would indicate a maximum difference of 2% Cr_2O_3 between the four crystals listed in Table 5.

The chemical analysis for Erzincan chlorite published by Lapham is

TABLE 5. REFRACTIVE INDICES ($\alpha \sim \beta \sim \gamma$)

Crystal	α at 589 mμ
1	1.6001
2	1.5976
3	1.5987
4	1.5995

given in Table 6*a*. Lapham (pers. comm., 1960) states that there are at least three Cr-chlorite localities in Erzincan province, so there is some question whether or not his material is identical with ours. A lack of agreement of the allocation from the published analysis with tetrahedral aluminum content as determined from T—O bond lengths for our crystal led to additional analyses of SiO_2, Al_2O_3, and Cr_2O_3. The revised analysis is given in Table 6*b*. We failed to get an accurate recheck on SiO_2 due to chromium interference in the procedure used. The value cited was obtained by difference. The Al_2O_3 content in our sample showed significant variation in different size fractions of the sample, but was always higher than that reported for Lapham's sample. The value reported in Table 6*b* is thought to be representative for our sample. Chromium analyzed by means of the *x*-ray spectrograph is also significantly higher than that reported by Lapham. The water content, rechecked by sample ignition and capture of vapor in P_2O_5, is lower, more in accord with the normal water content of chlorite. Finally, the CaO content reported by Lapham was not used in allocation because calcite does occur with this sample and it was thought likely that the CaO was an impurity. Belov (1950) has suggested that Ca could be incorporated in the chlorite structure in octahedral coordination between the talc and brucite sheets. There is no evidence from the electron density maps to support this suggestion for our sample.

TABLE 6. CHEMICAL ANALYSES

	SiO_2	Al_2O_3	Fe_2O_3	FeO	Cr_2O_3	MgO	CaO	H_2O^+	H_2O^-	Total
a)	32.2	8.7	0.5	1.4	6.5	31.5	1.0	13.8	0.6	99.8%
b)	31.4	10.0	0.5	1.4	9.3	35.1	—	12.3	—	100.0%

c) $Mg_{5.0}Ca_{0.1}Fe_{0.1}^{2+}Cr_{0.5}Al_{0.1})_{5.8}(Si_{3.1}Al_{0.9})_{4.0}O_{18}H_{8.8}$

d) $(Mg_{5.0}Fe_{0.1}^{2+}Cr_{0.7}Al_{0.2})_{5.0}(Si_{3.0}Al_{1.0})_{4.0}O_{18}H_{7.9}$ F. W. = 576.1

a) Analysis taken from Lapham (1958).

b) Modification of analysis (a) using new data for Al_2O_3, Cr_2O_3, and H_2O, excluding CaO as an impurity, and adding sufficient SiO_2 to total 100%.

c) Structural formula from analysis (a) on the basis of 18 oxygens per half-cell.

d) Structural formula from analysis (b) on the basis of 18 oxygens per half-cell.

Allocation of the revised chemical analysis yields a tetrahedral composition of Si_3Al. This composition was kindly confirmed for us by Dr. R. J. P. Lyon, Stanford Research Institute, who determined a tetrahedral Al value of approximately 1.0 from the shape of the infrared absorption bands in the 10 micron region (Tuddenham and Lyon, 1950). This value is considered representative of the bulk sample, although it is believed that individual crystals show compositional deviations. The measured and calculated densities for the bulk sample agree quite closely, $D_m = 2.702$ and $D_x = 2.706$ g/cm^3 respectively. The measured density is an average of four values obtained for different crystals, using a Berman balance and iso-amyl iso-valerate as the displacement medium.

Silicon-aluminum ordering An attempt was made to analyze statistically the significance of the differences in the average bond lengths of the T_I and T_{II} tetrahedra (Table 3). The standard deviations of the errors in peak positions of the tetrahedral Si, Al atoms and of the oxygens were derived from the ρ_o-ρ_c maps, using the relation given by Lipson and Cochran (1953)

$$\sigma_x = \left\{\left[\frac{\partial(\rho_o - \rho_c)}{\partial x}\right]^2\right\}^{1/2} \Big/ C \qquad (5)$$

where C is the central curvature of the ρ_o peak. The standard deviation of the T—O bond length is derived from the positional standard deviations of Si, Al and of oxygen by the relation

$$\sigma(T—O) = \{[\sigma_x(T)]^2 + [\sigma_x(O)]^2\}^{1/2}. \qquad (6)$$

The standard deviation of the error of an individual T—O bond in Erzincan Cr-chlorite is 0.02 Å (Table 3) and the standard error of the mean of the four tetrahedral distances,

$$\sigma_n = \frac{\sigma(T—O)}{\sqrt{n}},$$

is 0.01 Å. Cruickshank (1949) suggests that two bond lengths should differ by more than three standard deviation units in order to be considered real. For Cruickshank's test the standard deviation unit to be used for comparing tetrahedral means is

$$\sigma = \{[\sigma_n(T_I)]^2 + [\sigma_n(T_{II})]^2\}^{1/2}, \quad \text{or} \quad \sigma = \sqrt{n}\cdot\sigma_n$$

in the present case where the standard errors of the two tetrahedral means are the same. Thus, for Erzincan Cr-chlorite

$$\frac{\Delta(T—O)}{\sigma} = \frac{0.049}{0.01414} = 3.5.$$

According to this test the difference is real and the T_I tetrahedron is enriched in aluminum.

Smith (1954) has published a graph in which the mean T—O bond length was shown to vary linearly with tetrahedral Si, Al composition. The bond lengths Si—O = 1.60 Å and Al—O = 1.78 Å were considered to be the best values available for the end points. Advances in computing techniques since that time have made possible more accurate structure determinations, and it is now evident that the effect of external cations on individual T—O bond lengths is appreciable and that the mean T—O distance increases with a decrease in the number of shared corners (Smith and Bailey, 1963). Therefore separate mean T—O graphs are required for each linkage type. Standard values Si—O = 1.62 Å and Al—O = 1.77 Å are suggested for layer silicates, in which the mean of all four bond lengths must be used because of the change in shape of the tetrahedra due to changes in composition. These revised values applied to the Erzincan chlorite T—O lengths indicate a composition $Si_{2.92}Al_{1.08}$ for four tetrahedral sites.

T_I—O:	1.685 Å	equivalent to 0.57 Si,	0.43 Al
T_{II}—O:	1.636 Å	equivalent to 0.89 Si,	0.11 Al

This tetrahedral composition is intermediate between the $Si_{3.0}Al_{1.0}$ allocation resulting from chemical analysis and infrared study of the bulk sample and the value $Si_{2.8}Al_{1.2}$ indicated for the crystal by the observed basal oxygen-oxygen distances relative to the graph of Fig. 5.

Chromium ordering. The structural formula derived from the chemical analysis indicates 0.7 atoms of Cr per six octahedral positions. Lapham (1958) suggests, on the basis of 001 and 003 intensity calculations, that the Cr in his Erzincan sample is concentrated in the brucite sheet. A similar result is obtained for our sample by using the intensities of the basal reflections with $l = 2n+1$, as suggested by Brindley and Gillery (1956), and by constructing a one-dimensional electron density projection onto [001]. The two-dimensional ρ_o-ρ_c and ρ_o electron density maps indicate the Cr is segregated preferentially in one site within the brucite sheet on a center of symmetry (M_{IV} site). This is confirmed by the smaller size of the metal-hydroxyl distances in the M_{IV} site as compared to the M_{III} site (Table 3). The magnitude of the difference, 0.057 Å, suggests that the 0.2 atoms of Al allocated to octahedral sites are also concentrated in the M_{IV} site to give complete ordering of divalent and trivalent cations. We have been unable to locate specifically the 0.1 atoms of octahedral Fe indicated by chemical analysis. The difference in sizes of the brucite M_{III} and M_{IV} octahedra is real, according to Cruickshank's criteria, whereas the minor differences between the M_I and M_{II} talc octahedra and between these and the M_{III} brucite octahedron are not significant. The brucite

sheet is slightly thinner on the average than the talc octahedral sheet, 2.03 Å relative to 2.15 Å.

In the Erzincan chlorite the excess negative charge due to the substitution of Al for Si in the tetrahedral sheets is compensated entirely by substitution within the brucite sheet. The M_{IV} brucite position in the I*a*-4 polytype is located exactly between the T_I positions in the tetrahedral sheets above and below. As a result, the locus of excess positive charge on the brucite sheet due to concentration of trivalent Cr and Al in site M_{IV} is in closest possible approach to the excess negative charges on the Al-rich T_I tetrahedra. The M_{III} brucite site, on the other hand, is positioned vertically between a T_{II} site and the center of a ditrigonal oxygen ring. As a result the M_{III} cation is repelled slightly away from the Si in T_{II} and towards the ring opening. The I*a*-4 (or the equivalent I*a*-6) polytype is ideally adapted for local charge balance of this sort because the symmetry allows all of the trivalent ions to be concentrated in the one brucite position that lies between tetrahedral sites above and below. This is not true for the I*a*-2structure, which has two such brucite sites and would require a different and less efficient ordering scheme.

Stability. Theoretically one might expect that a polytype such as I*a*-4, which permits vertical superposition of brucite and tetrahedral cations, would be an unstable, high energy structure. The cation outer surfaces are separated by less than 3.5 Å and are incompletely screened by the intervening oxygen and hydroxyl anions. It was pointed out in Part I that the I*a* and II*a* layer types, which have the greatest amount of cation superposition, are comparatively rare, at least for chlorites in the Mg-Fe system. The observed rarity may be a consequence of the cation repulsion inherent in these structures. The I*a* layer is characteristic, however, of the structures of vermiculite and of the Li-Al chlorite, cookeite.

We believe that the unfavorable aspect of repulsion between the tetrahedral and brucite cations is compensated in the case of the Erzincan Cr-chlorite by the cation ordering scheme which permits local satisfaction of the excess negative and positive charges on the talc and brucite sheets. It is hoped that further evidence regarding the importance of this local charge balance will be obtained from the structure refinement of I*a* cookeite that is now being started. The stability of the I*a* structure is enhanced in the case of vermiculite by occupation of only $\frac{1}{9}$ of the available brucite cation sites, which reduces considerably the total amount of cation repulsion. It should be noted also that the I*a* and II*b* layers are the only arrangements of chlorite sheets in which it is possible to rotate the tetrahedra so that the basal oxygens approach more closely both the adjacent brucite hydroxyl surfaces and the talc octahedral cations. This is possible

because the hydroxyls in the lower plane of the brucite sheet project along the normal to the sheet directly onto the octahedral talc cations below. The basal tetrahedral oxygens lie between the levels of the talc octahedral cations and the brucite hydroxyls but to one side, and shift towards them by the mechanism of tetrahedral rotation (Fig. 4). A similar geometric alignment is observed in the structures of kaolinite and dickite. The sequence of sheets in the I*b* and II*a* chlorite layers, however, is such that the brucite hydroxyls do not superimpose on the talc octahedral cations. The structure determination of an orthohexagonal I*b* chlorite, now in progress, should prove by the observed direction of rotation of tetrahedra whether the basal tetrahedral oxygens are attracted more by the talc cations or by the bond to the brucite sheet.

Acknowledgements

This study was supported in part by the Research Committee of the Graduate School from funds supplied by the Wisconsin Alumni Research Foundation. Participation of the senior author was made possible by a National Science Foundation postdoctoral fellowship. Computations were carried out in the University of Wisconsin Numerical Analysis Laboratory, which has also benefited from National Science Foundation support. We wish to express our appreciation to Dr. R. A. Bell for providing the crystals on which the study was made, to Dr. D. M. Lapham for providing a comparison sample from Erzincan and for discussions in regard to this sample, to Dr. H. H. Bostock and Mr. G. L. LaBerge for the refractive index measurements, and to Dr. R. J. P. Lyon for the infrared pattern.

References

Bailey, S. W. and B. E. Brown (1962) Chlorite polytypism: I. Regular and semi-random one-layer structures. *Am. Mineral.*, **47**, 819–850 .

Belov, N. V. (1950) Research in the field of structural mineralogy. *Min. Sbornik, Lvov*, **4**, 21–34.

Berghuis, J., I. M. Haanappel, M. Potters, B. O. Loopstra, C. H. MacGillavry, and A. L. Veenendaal (1955) New calculations of atomic scattering factors. *Acta Cryst.* **8**, 478–483.

Bradley, W. F. (1959) Current progress in silicate structures. *Clays and Clay Minerals, 6th Nat. Conf.*, 18–25.

Brindley, G. W. and F. H. Gillery (1956) *X*-ray identification of chlorite species. *Am. Mineral.* **41**, 169–186.

——— Beryl M. Oughton and K. Robinson (1950) Polymorphism of the chlorites. I. Ordered structures. *Acta Cryst.* **3**, 408–416.

——— and K. Robinson (1951) The chlorite minerals, p. 173–198 in *X-ray Identification of Clay Minerals*. Mineral. Soc., London.

Cruickshank, D. W. J. (1949) The accuracy of electron-density maps in *X*-ray analysis with special reference to dibenzyl. *Acta Cryst.* **2**, 65–82.

DRITS, V. A. AND A. A. KAESHAEV (1960) An *X*-ray study of a single crystal of kaolinite. *Soviet Physics—Crystallography* (Eng. transl.), **5,** 207–215.

GARRIDO, J. (1949) Structure cristalline d'une chlorite chromifère. *Bull. Soc. Franc. Miner. Crist.* **72,** 549–570.

HOWELLS, E. R., D. C. PHILLIPS AND D. ROGERS (1950) The probability distribution of *X*-ray intensities. II. Experimental investigation and the *X*-ray detection of centres of symmetry. *Acta Cryst.* **3,** 210–214.

LAPHAM, D. M. (1958) Structural and chemical variation in chromium chlorite. *Am. Mineral.* **43,** 921–956.

LIPSON, H. AND W. COCHRAN (1953) *The Determination of Crystal Structures.* London, G. Bell and Sons.

MATHIESON, A. MCL. (1958) Mg-vermiculite: a refinement and re-examination of the crystal structure of the 14.36 Å phase. *Am. Mineral.* **43,** 216–227.

MCMURCHY, R. C. (1934) The crystal structure of the chlorite minerals. *Zeit. Krist.* **88,** 420–432.

NEWNHAM, R. E. (1961) A refinement of the dickite structure and some remarks on polymorphism in kaolin minerals. *Mineral. Mag.* **32,** 683–704.

PAULING, L. (1930), The structure of the chlorites. *Proc. Nat. Acad. Sci.* **16,** 578–582.

RADOSLOVICH, E. W. (1960) The structure of muscovite, $KAl_2(Si_3Al)O_{10}(OH)_2$. *Acta Cryst.* **13,** 919–932.

——— (1961) Surface symmetry and cell dimensions of layer lattice silicates. *Nature,* **191,** 67–68.

SMITH, J. V. (1954) A review of the Al-O and Si-O distances. *Acta Cryst.* **7,** 479–481.

——— AND S. W. BAILEY (1963) Second review of Al-O and Si-O tetrahedral distances. *Acta Cryst.* (in press).

STEINFINK, H. (1958a) The crystal structure of chlorite. I. A monoclinic polymorph. *Acta Cryst.* **11,** 191–195.

——— (1958b) The crystal structure of chlorite. II. A triclinic polymorph. *Acta Cryst.* **11,** 195–198.

——— (1961) Accuracy in structure analysis of layer silicates: Some further comments on the structure of prochlorite. *Acta Cryst.* **14,** 198–199.

——— AND G. BRUNTON (1956) The crystal structure of amesite. *Acta Cryst.* **9,** 487–492

TAKÉUCHI, Y. AND R. SADANAGA (1959) The crystal structure of xanthophyllite. *Acta Cryst.* **12,** 945–946.

TUDDENHAM, W. M. AND R. J. P. LYON (1959) Relation of infrared spectra and chemical analysis for some chlorites and related minerals. *Analyt. Chem.* **31,** 377–380.

WEISZ, O., W. COCHRAN AND W. F. COLE (1948) The accurate determination of cell dimensions from single-crystal *X*-ray photographs. *Acta Cryst.* **1,** 83–88.

WILSON, A. J. C. (1949) The probability distribution of *X*-ray intensities. *Acta Cryst.* **2,** 318–321.

——— (1951) Variance of *X*-ray intensities. *Research,* **4,** 141–142.

Manuscript received July 26, 1962; accepted for publication, November 1, 1962.